

Superconductivity and Quantum Oscillations in Crystalline Bi Nanowire

Mingliang Tian,^{*,†,‡} Jian Wang,^{*,†,‡} Qi Zhang,^{†,§} Nitesh Kumar,^{†,‡}
Thomas E. Mallouk,^{†,‡,||} and Moses H. W. Chan^{*,†,‡}

Center for Nanoscale Science (CNS), Department of Physics, Materials Research Institute (MRI), Department of Chemistry, the Pennsylvania State University, University Park, Pennsylvania 16802-6300

Received May 5, 2009

ABSTRACT

While bulk bismuth (Bi) is a semimetal, we have found clear evidence of superconductivity in 72 nm diameter crystalline Bi nanowire below 1.3 K. In a parallel magnetic field (H), the residual resistance of the nanowire below T_c displays periodic oscillations with H , and the period corresponds to a superconducting flux quantum. This result indicates that the superconductivity originates from the cylindrical shell between Bi inner core and the surface oxide layer. Under a perpendicular H , the resistance in the superconducting state shows Shubnikov–de Haas (SdH)-like oscillations, a signature of a normal metal. These results suggest a novel coexistence of superconducting and metallic states in the temperatures well below T_c .

The electronic properties of bismuth (Bi) have been extensively studied for almost a hundred years. Its extremely small Fermi surface (FS) (just 10^{-5} of the Brillouin zone), low carrier density ($\sim 3 \times 10^{17}/\text{cm}^3$ at 2 K), small effective carrier mass ($m_e^* < 0.003 m_0$ for electrons along the trigonal direction)^{1,2} and very long electron mean free path (exceeding $2 \mu\text{m}$ at room temperature)^{3,4} distinguish Bi from other metals as particularly suitable for studying quantum phenomena.^{5,6} Recent studies on this “old” material has found a number of new phenomena,^{7–9} such as the one-dimensional topological metal states at the surface and on the edges of a Bi crystal,⁷ the bulk Dirac particles,⁸ and the charge quantum Hall fractionalization in the quantum limit.⁹ Metallic surface states are a prerequisite for the formation of a topological insulator¹⁰ and are analogues to the edge states of a quantum spin Hall insulator,¹¹ which has been naturally realized in Sb-doped Bi bulk.¹² These new findings suggest that this old material may have potential application in developing next-generation quantum computing devices that incorporate “light”-like bulk carriers and spin-textured surface currents.¹²

Compared to the semimetallic bulk system, single-crystal Bi nanowire of several tens of nanometers was predicted to be a semiconductor by band structure calculation.¹³ In fact, the electronic properties of Bi nanowires were found to be more complex,^{14–22} sensitively depending on the details of

wire dimension, morphology, and even the growth orientation. There is evidence that the transport behavior of Bi nanowires is dominated by surface effects. In 55 and 75 nm single-crystalline Bi nanowire arrays, Nikolaeva et al.¹⁵ observed Aharonov–Bohm (AB)-type²³ magnetoresistance oscillations due to quantum interference of phase coherent electrons along the bifurcating trajectories on the highly conducting surface of the wire. In an ultrathin 30 nm diameter nanowire array, Huber et al.¹⁶ found isotropic Shubnikov–de Haas (SdH) oscillations in contrast to the ordinarily anisotropic SdH oscillations in bulk Bi. This led the authors to propose a scenario in which the 30 nm Bi nanowire is metallic in its entire volume with a spherical FS due to surface states, which inhibits the semimetal to semiconductor transition. Interestingly, when the nanowires were made in the form of granular morphology with a grain size of 10–15 nm, fabricated by electrodepositing Bi into porous membranes, the granular nanowire arrays show superconductivity with a T_c of 7.2 or 8.3 K.^{21,22} These T_c 's coincide with those of high-pressure phases, Bi-III and Bi-V,²⁴ and therefore were attributed to a consequence of the distorted interfacial structures between the grains. Because the surfaces of Bi nanowires are always oxidized when they are released from the porous membrane, most of previous transport measurements were carried out on Bi nanowire arrays still embedded inside the porous membranes with two-lead configuration,^{13–22} and the working temperature is above 2.0 K.^{13–20}

In this paper, we report a systematic study of the transport properties of individual crystalline Bi nanowire of 72 nm diameter in the temperature range between 0.05 and 300 K,

* To whom correspondence should be addressed. E-mail: (M.T.) tian@phys.psu.edu; (J.W.) juw17@psu.edu; (M.H.W.C.) chan@phys.psu.edu.

† Center for Nanoscale Science (CNS).

‡ Department of Physics.

§ Materials Research Institute (MRI).

|| Department of Chemistry.

with standard four-lead configuration. Remarkably, we found evidence that the Bi nanowire displays superconductivity below 1.3 K. Under a parallel magnetic field \mathbf{H} , the residual resistance of the wires shows periodic oscillations with \mathbf{H} well in the superconducting state, that is, $T < 0.8$ K. The period of the oscillations corresponds to the superconducting flux quantum, $\Phi_0 = h/2e = 2.07 \times 10^{-7}$ G cm² (here e is the electron charge and h is Plank's constant), reminiscent of Little–Parks (LP) oscillations in a “hollow” superconducting cylinder.²⁵ The LP-like oscillations unambiguously suggest that the observed superconductivity in Bi nanowire originates from the cylindrical shell between the inner core of the Bi nanowire and its surface oxide. LP oscillations were observed previously in hollow AuIn and Al cylinders with diameter as small as 150 nm.²⁶ We show here that the LP phenomenon is realized in a shell of only 72 nm. However, when the field is aligned perpendicular to the wire axis, the residual resistance below 0.8 K still shows oscillations with varying \mathbf{H} . Interestingly, the oscillations at $\mathbf{H} > 7.5$ kOe appear to be periodic with $1/\mathbf{H}$ instead of \mathbf{H} . The $1/\mathbf{H}$ periodicity of the residual resistance oscillations is suggestive of the SdH effect due to the Landau quantization of the orbiting Fermi quasi-particle energy of a metal. The SdH behavior in the superconducting state is not expected.

The nanowires were fabricated by electrochemically depositing Bi into custom-made porous anodic aluminum oxide membranes.²⁷ The electrolyte was prepared as the following: 10 g/L BiCl₃ + 50 g/L NaCl + 50 g/L tartaric acid + 100 g/L glycerol.²⁸ The milky aqueous solution was then made clear by adjusting the pH to 1–2 with concentrated hydrochloric acid (HCl). The electrodeposition was carried out at a constant potential of -0.18 V, relative to an Ag/AgCl reference electrode at room temperature. A pure Pt wire was used as the positive counter electrode and an Ag film, evaporated onto one side of the membrane prior to the deposition was used as the working electrode. Free standing nanowires were obtained by dissolving the membrane with 2 M aqueous NaOH solution, followed by precipitating the wires via centrifugation. The nanowires were stored as a suspension in ethanol prior to structural imaging by transmission electron microscopy (TEM) and electrical transport measurements.

Figure 1a shows low-magnification TEM image of Bi nanowires dispersed on the TEM grid. We usually start with a quick check on the uniformity and morphology of typically hundreds wires dispersed on the TEM grid. After the quick examination, we typically study 15–20 wires systematically at different magnifications before picking 3–4 wires for careful electron diffraction studies including the recording of high resolution images. Figure 1b shows an enlarged TEM image of a randomly selected Bi nanowire. The nanowire, including the oxide layer, has a diameter of 79 nm and displays a bamboo-like morphology along its length, as indicated by the arrows. The wire diameter varies typically less than 5% along its entire length of each wire. The variation in the diameter from wire to wire is typically less than 10%. A high resolution TEM image (Figure 1c) taken near the “bamboo” stripe indicated that the stripes shown in

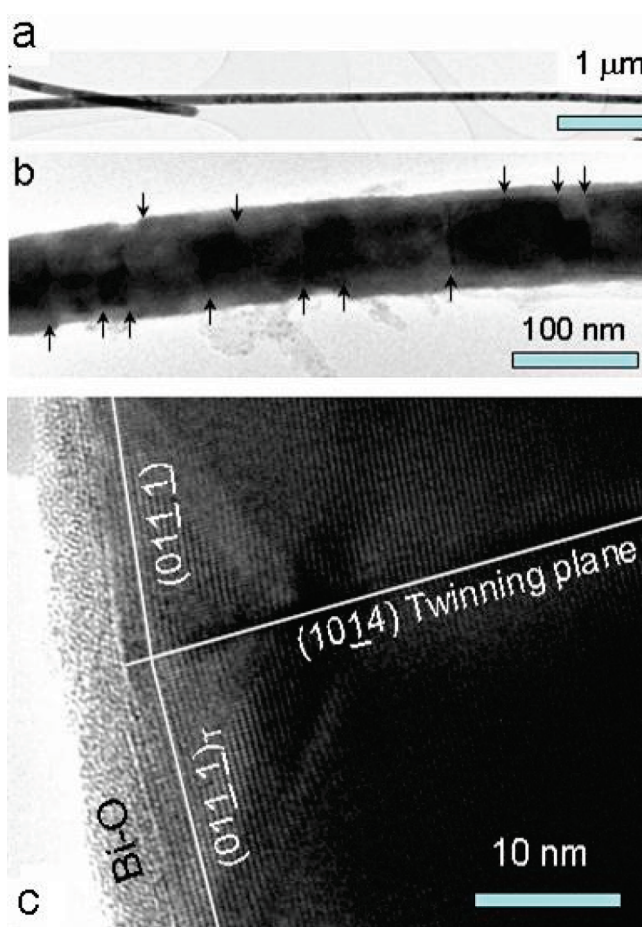


Figure 1. TEM images of Bi nanowires. (a) Low magnification; (b) enlarged image showing bamboo-like stripes along the length, as indicated by the arrows; (c) HRTEM image near one of these stripes, indicating that the stripes are actually (1014) twinning boundary, which is perpendicular to the growth direction.

Figure 1b are actually small-angle twinning boundaries with a twinning plane of (1014), which is perpendicular to the growth direction of the wire. The length of each single-crystal segment between two neighboring twinning planes can be as short as 20 nm and up to a few hundred nanometers in the wire. This result was confirmed by X-ray diffraction (XRD) measurements on Bi wire arrays, where the (104) diffraction is the dominant peak in the spectra. Stress fringes near each twinning plane were noticed in the vicinity of the surface, indicating a lattice strain at surface of the wire that is released in the inner core. An oxide layer of approximately $\sim 3.7 \pm 0.5$ nm, probably formed after the nanowires were released from the membrane, is visible on the surface. Therefore, the actual inner diameter (d) of the Bi nanowire inside the oxide shell is about 72 nm. While the twinning boundaries may have a similar role as grain boundaries in granular wires, we call these bamboo-like twinned wires “crystalline” wires in order to discriminate them from typical granular wires where the size of the spherical grains is smaller than the wire diameter and the orientation of the grains are mostly random.^{21,22}

Standard 4-probe transport measurements were carried out on four similarly fabricated individual Bi nanowires, harvested from four different membranes (we call them samples

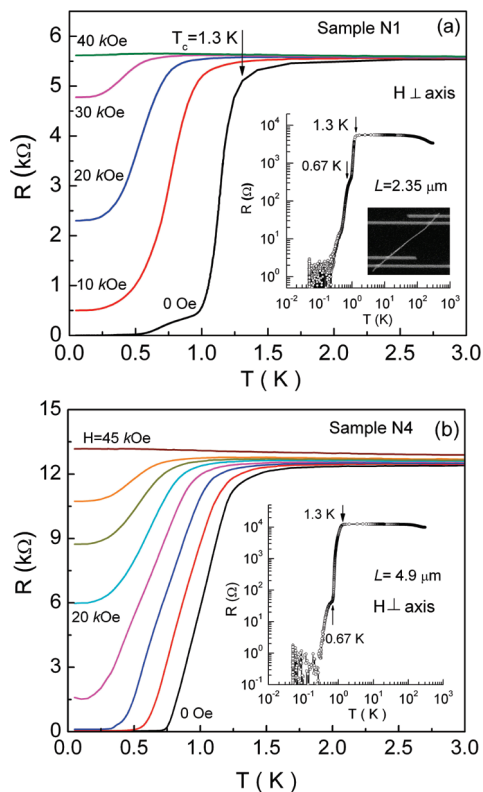


Figure 2. R vs T curves of (a) samples N1 and (b) N4, respectively, measured under different perpendicular magnetic fields. The inset in each plot shows the R – T curve at $\mathbf{H} = 0$ Oe in log–log scale. A superconducting transition was found at 1.3 K in both samples. Four-lead configuration of N1 deposited by FIB technique is shown in the inset of (a).

N1, N2, N3, and N4) of the same pore diameter in a physical property measurement system (PPMS) cryostat equipped with a dilution refrigerator insert and a 9 T superconducting magnet. Four Pt strips of 100 (width) \times 100 (thickness) nm² were deposited onto the Bi nanowires as electrodes using the focused-ion beam (FIB) technique (see inset of Figure 2a).²⁹ It was found that the insulating Bi–O oxide layer covering the Bi wire is reliably penetrated by the deposition of Pt electrodes and an ohmic contact can be obtained between the Pt lead and the Bi wire. This was confirmed by linear V – I characteristics in the normal state of the wire. The maximum spreading distance of Pt composite along the nanowires was found to be less than 300 nm beyond the intended position through a profile analysis of the TEM energy dispersive X-ray spectra. For all four samples, the distance (L) between the inner edges of the two voltage Pt electrodes was kept larger than 2.0 μm .

Resistance (R) versus temperature (T) curves of samples N1 ($L = 2.35 \mu\text{m}$) and N4 ($L = 4.9 \mu\text{m}$) in temperature range of 0.05–300 K are shown in the inset of Figure 2a,b, respectively. The nanowires display a semiconducting-like behavior from room temperature down to 40 K. The measured resistivities of N1 and N4 at room temperature are respectively 582 and 814 $\mu\Omega\cdot\text{cm}$, which is 5.5 and 7.7 times larger than its bulk value ($\rho_{\text{bulk}} = 106 \mu\Omega\cdot\text{cm}$) and on the order as that reported by Conelius et al.³⁰ Just below 1.3 K, the resistance of the nanowire shows a sharp drop,

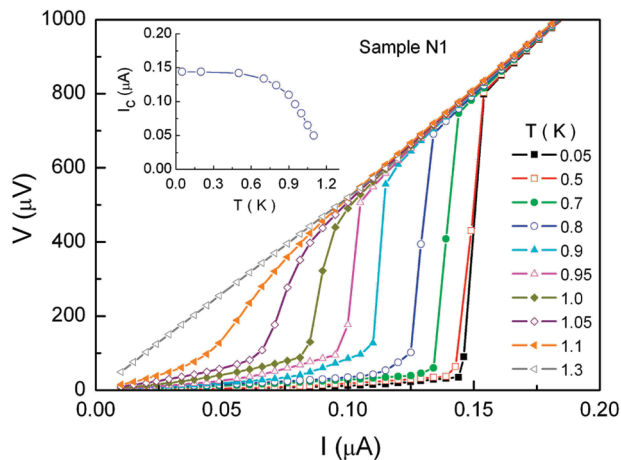


Figure 3. V – I curves for sample N1 at different temperatures. Inset shows I_c – T dependence.

decreasing by 3 orders of magnitude and eventually reaching a value beyond the resolution of our system below 0.3 K. The log R –log T plot in the inset of Figure 2a,b shows a shoulder around 0.67 K. The resistance drop at the shoulder is only about 4% of its normal state resistance R_N at 1.3 K in N1 and 0.3% R_N in N4.

By applying a perpendicular \mathbf{H} , the transition temperature of both samples was pushed to low temperatures and finally below 50 mK at 40 kOe, as shown in Figure 2a,b. The shoulders in both samples were suppressed at a field larger than 10 kOe. The 3 orders of magnitude drop in R down to zero is a clear signature of a superconducting transition.

Figure 3 shows voltage–current (V – I) characteristics of sample N1, measured at different temperatures. At 50 mK, a sharp discontinuous jump in voltage was seen at 0.14 μA (0.12 μA in N4). This value corresponds to a superconducting critical current density of $j_s = 3.4 \times 10^3 \text{ A/cm}^2$ if we assume that the current passes uniformly through the entire cross-section area of the wire. This value is 2 to 3 orders of magnitude smaller than that observed in typical superconducting nanowires ($j_s \sim 10^5$ – 10^6 A/cm^2 in Sn, Nb, and Al nanowires) at nearly the same temperature.^{31–33} The critical current decreases with increasing temperatures and the crossover from superconducting to normal state becomes more rounded.

A signature of superconductivity in “crystalline” Bi nanowires still embedded in a porous polycarbonate membrane was seen at 0.64 K by Ye et al.³⁴ In the experiment of Ye et al., zero resistance was not found and the wire resistance drops by 30% of its normal state value between 0.64 K and 50 mK. The shoulder around 0.67 K in N1 and N4 is likely related to the same superconducting phase observed by Ye et al. The critical magnetic field (\mathbf{H}_c) of this superconducting phase was found to be around 7.0 kOe in ref 34, which is also consistent with that found in our wires. To our knowledge, the result of ref 34 is the only other experimental evidence showing superconductivity in small diameter crystalline Bi nanowires.

R versus \mathbf{H} isotherms of N1 measured with \mathbf{H} aligned parallel and perpendicular to the wire axis are shown in

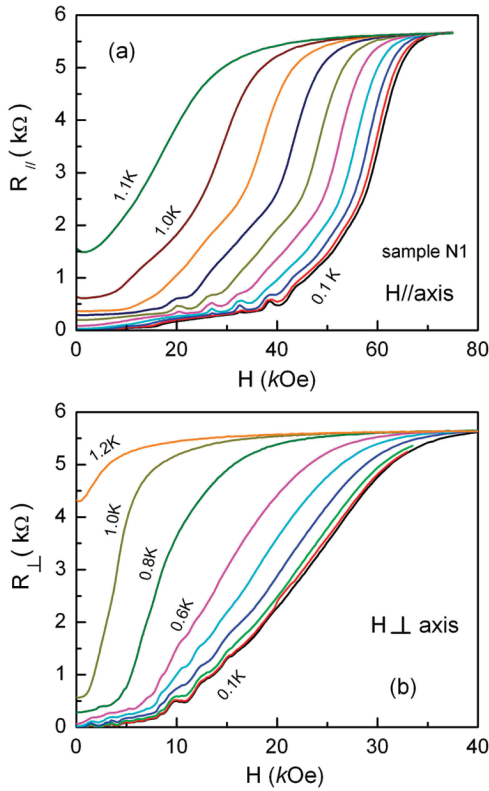


Figure 4. R – H plots for sample N1 at different temperatures for magnetic fields: (a) applied parallel to the wire axis; (b) applied perpendicular to the wire axis.

Figure 4a,b, respectively. The nanowire exhibits strong anisotropic magnetic behavior with a broad resistive transition from the superconducting to the normal state. If we define the point at which the resistance of the nanowire is restored to 98% of its normal state value as “the critical field”, the magnitude of the perpendicular critical field at 0.1 K, $H_{ct} \sim 34$ kOe, is approximately one-half of the parallel critical field, $H_{cp} \sim 67$ kOe. This demagnetization effect is consistent with the expectation for a thin superconducting cylinder.³⁵ These critical fields at 34 and 67 kOe are attributable to the 1.3 K phase because the 0.67 K phase has been suppressed at 10 kOe.

The most remarkable feature of Figure 4a,b is the series of resistance oscillations observed at magnetic fields and temperatures well below their critical values. To show clearly the resistance oscillations, a smooth R vs H background was subtracted from each of the R – H isotherms. The subtracted curves $\Delta R_{||}$ at different temperatures show oscillations periodic with H (Figure 5 a). The vertical dashed lines, separated from each other by $\Delta H = 5.85$ kOe are found to locate the majority of the local minima of the $\Delta R_{||}$ – H isotherms. For the $T = 0.5$ K isotherm, 5 minima are pinpointed by the dashed lines. At higher temperatures the oscillations in R extend to lower H but become difficult to resolve at higher fields. For $T < 0.4$ K, the first broad peak near 11.7 kOe is not related to the same set of the oscillations but originates from the suppression of the superconductivity of the 0.67 K phase in parallel H . Some additional peaks that deviate from the periodicity of the set of the oscillations show up at fields above 40 kOe.

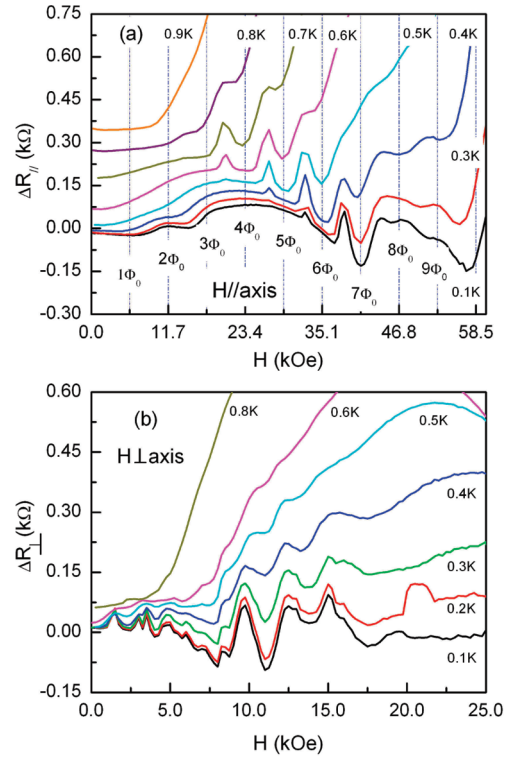


Figure 5. (a) $\Delta R_{||}$ – H and (b) ΔR_{\perp} – H plots, obtained by subtracting smooth background from the data in Figure 4a,b. Periodic oscillations of R were clearly seen in parallel H , and the dashed lines in panel a indicate the positions of fluxoid quantization as predicted by $H(\pi d^2/4) = n\Phi_0$ with $d = 67$ nm. In perpendicular H , the R –oscillations are more complex without recognized periodicity.

In a superconducting system, the oscillations of resistance as a function of external magnetic field are expected in either small superconducting hollow cylinder²⁵ or disk^{36–38} when the shell thickness of the hollow cylinder or the size of the disk is comparable to the superconducting phase coherence length. This phenomenon, named the Little–Parks (LP) effect²⁵ is a consequence of “fluxoid” quantization.^{25,36–40} The standard LP oscillations in a small hollow cylinder are characterized by the integer multiples of the superconducting flux quantum, Φ_0 , that is, $H(\pi d^2/4) = n\Phi_0$, where d is the diameter of the hollow cylinder and n is an integer. In this model, $\Delta H = 5.85$ kOe results in $d = 67.0$ nm. This value is close to 72 nm, the nominal wire diameter as determined by TEM.

In contrast to the hollow cylinder LP effect, the oscillations in a small disk are pseudoperiodic with flux quanta and the period which is mostly larger than Φ_0 decreases smoothly with increasing H .^{38–40} The oscillations correspond to transition between the quantum states with different angular momentum L (L also corresponds to the number of vortices inside the disk). The reason why the oscillation is not strictly periodic with H is partly due to the changing configurations of vortices inside the disk since the quantized vortices can merge into clusters or even forming giant vortex induced by pinning.⁴¹ One possible scenario is that the observed superconductivity originated from the (1014) twinning planes and there is a series of superconducting disks along the wire which contribute to the LP oscillations. 2D twinning plane

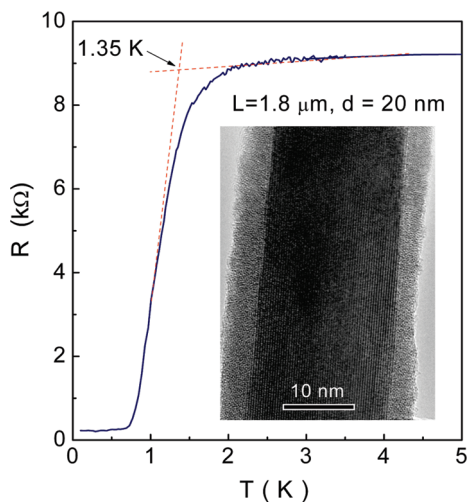


Figure 6. R vs T curve of 20 nm diameter Bi wire. A resistance drop is seen around 1.35 K but with a finite resistance down to 50 mK. The inset is a HRTEM image of the wire, indicating a single-crystal morphology without twinning planes. The actual diameter of the wire including the surface oxide is 28 nm.

superconductivity has been proposed theoretically and experimentally observed in Al, In, and Sn twinning crystals.^{42–44} There is strong evidence that the 1.3 K superconducting phase is not related to the twinning planes. In addition to Bi wires of 72 nm, we have also made measurements on 20 nm diameter single-crystal Bi nanowires (28 nm including the surface oxide layer). In contrast to the 72 nm wires, the 20 nm wires are single-crystal without twinning planes as shown in the inset of Figure 6. The R – T result of the 20 nm wire (see Figure 6) shows a superconducting transition near 1.35 K similar to that found in 72 nm wire without evidence of another superconducting drop at 0.67 K. The 20 nm diameter wire does not show LP oscillations in parallel \mathbf{H} ; this is because the expected period of the LP oscillations is 65.8 kOe, which is on the order of the critical field of the wire. The detailed results in ultrathin Bi wires will be published elsewhere. This would suggest the 1.3 K superconducting phase is not related to the twinning planes. On the other hand, the 0.67 K superconducting phase shown in Figure 2 and ref 34 could have its origin of superconductivity from the twinning planes. Since the critical field of the 0.67 K phase is on the order of 10 kOe but the LP oscillations are observed well above 10 kOe and at temperatures above 0.7 K, the LP oscillations shown in Figure 5a must have their origin from the 1.3 K phase.

The fact that the minima of ΔR_{\parallel} in an individual wire nicely coincide with integer multiples of the superconducting flux quantum, Φ_0 , that starts with $\mathbf{H} = 0$ Oe and with d equals to the actual wire diameter as determined by TEM are strong evidence that the 1.3 K superconducting phase in these twinning Bi nanowires is likely due to a thin cylindrical shell in the BiO_x/Bi interface. In a prior transport measurements on an ensemble of single-crystalline Bi nanowires of 20 and 70 nm still imbedded inside the membrane, no evidence of superconductivity was found down to 0.47 K.²¹ When the wires are still embedded in the membrane, there will not be an oxide layer on the surface of the wires. This

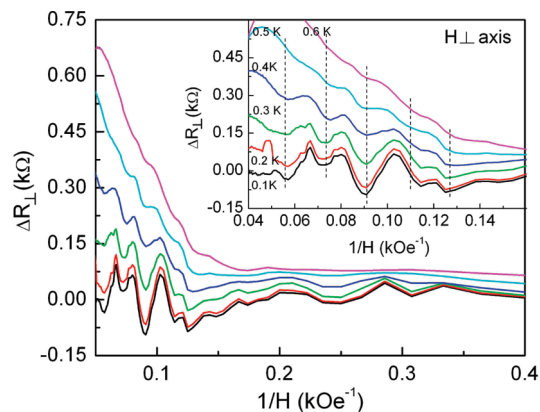


Figure 7. ΔR_{\perp} – $1/\mathbf{H}$ curves deduced from the data in Figure 5b. The inset shows the blow-up of the plot in the field regime, $\mathbf{H} > 7.5$ kOe. Quasi-periodic oscillations of R with $1/\mathbf{H}$ are clearly seen, especially for the curves at 0.4 and 0.5 K. Dashed lines, separated by $\Delta(1/\mathbf{H}) = 0.0176$ kOe^{–1} show good correlation with the minima of resistance oscillations as predicted by the SdH effect.

result also supports the interpretation that the 1.3 K superconducting phase observed in an individual wire originates from the interface between the surface oxide and the inner core of the Bi wire.

Standard LP oscillations in a superconducting hollow cylinder are expected in the R – \mathbf{H} curves near T_c or \mathbf{H}_c . A significant deviation here is that the oscillations are observed deep in the superconducting state, far below 1.3 K and 67 kOe. The possible explanation is that the Bi nanowires reported here is no longer fully superconducting by the application of a parallel magnetic field. Even at $\mathbf{H} = 0$ Oe, the nanowires show a finite resistance between 0.3 and 1.3 K. The broadening and the finite resistance below the onset of superconducting transition are likely the consequence of size confinement in 1D created by phase slippage processes,^{45–48} such as thermally activated phase slips near T_c or the quantum phase slips far below T_c (in N1, the quantum phase slips-like resistive tail in $\log R$ – T curve was noticed below 0.67 K. Such a resistance tail was not seen in N4). Thus, as the magnetic field is increased at temperatures even well below T_c , one expects to see a crossover regime from predominantly superconducting to predominantly metallic state as shown in Figure 4a,b. Such a crossover regime is not the exact thermodynamic phase transition and there is no true critical magnetic field. In the superconducting-dominated states the magnetic field creates Meissner screening currents and through them suppresses the energy barrier for the phase slips. The observed resistance oscillations are likely the reflection of the oscillations of the screening currents as a function of the magnetic field.

Oscillations in resistance are also seen under a perpendicular field (Figure 4b). However, these oscillations are not periodic with \mathbf{H} (Figure 5b). Figure 7 shows ΔR_{\perp} – $1/\mathbf{H}$ curves and the inset is the blow-up of the plot in the field region $\mathbf{H} > 7.5$ kOe. The oscillations in ΔR_{\perp} appear to be periodic with $1/\mathbf{H}$ at least between 7.5 and 20.0 kOe. The vertical dashed lines in the inset drawn with a period of $\Delta(1/\mathbf{H}) = 0.0176$ kOe^{–1} pinpoint nicely the 5 local minima of the 0.4 and 0.5 K isotherms in this field range. For isotherms

below 0.4 K, the vertical line at $1/H = 0.115 \text{ kOe}^{-1}$ misses the minimum. Oscillations in R that are periodic with $1/H$ are characteristic signature of the SdH oscillations.^{4–6} As a result, the observation of the SdH oscillations is usually taken as clear-cut evidence for the existence of the FS and is unexpected for a system in the superconducting state.

It is tempting to explain the SdH effect not due to the superconducting interfacial shell but to the inner nonsuperconducting core (as noted above at a field of larger than $\sim 10 \text{ kOe}$, the 0.67 K phase nucleated at twinning planes has been suppressed). This speculation is however inconsistent with our experimental data. First, the parallel contribution of the semiconducting inner core to the total electrical conductance is negligibly small compared to that of the nearly fully superconducting shell. Thus, any variations or oscillations in the resistance of the inner core are not detectable far below H_c . Second, the SdH signatures were seen only deep in the superconducting state below 0.7 K. If the $1/H$ oscillations originate from the normal core, they should not be sensitive to the onset of superconductivity and should be observed both above and below T_c . The most reasonable explanation is that the SdH oscillations also have their origin from the same superconducting shell.

As we mentioned above, the LP oscillations most likely originate from the surface shell between surface oxide and the inner core of the wire. The finite resistance in the crossover regime from predominantly superconducting to predominantly metallic state is due to both the phase slips (PS) and the normal resistance of the Fermi quasi-particles, which is locally and temporarily realized as the normal core of the PS in the shell. The barriers to PS oscillate in H following LP oscillations of supercurrent and the normal resistance follows the SdH oscillations. In parallel H , the SdH oscillations were not resolved because the thickness of the superconducting cylindrical shell is too thin, only on the order of 2.5 nm (the d is 67 nm estimated from LP oscillations, 5 nm smaller than the diameter of the wire), which is smaller than the radius of the Landau orbit of cyclotrons ($>10 \text{ nm}$). The SdH oscillations were reported in some of highly anisotropic type-II superconductors in the reversible vortex states,^{49,50} where vortices are free to move and a finite resistance exists. A central feature in these systems is that the SdH was seen in both the superconducting and normal states with the same periodicity. The amplitude of oscillations in the superconducting phase showed a significant attenuation due to the opening of a superconducting gap. In our experiments, the $1/H$ oscillations in perpendicular H were found only deep in the superconducting phase far below 34 kOe. A possible reason might be that to reach the normal state, the magnetic field needs to be larger than the field at which the last wave of SdH is expected to occur.

For $H < 7.5 \text{ kOe}$, the R -oscillations are neither periodic with H or $1/H$. Resistance oscillations as a function of a perpendicular H have been reported in various superconducting nanostructures, such as Josephson junction arrays,⁵¹ 1D nanowire,^{52,53} nanoribbon,⁵⁴ and nanobelt.⁵⁵ The oscillations were interpreted as a consequence of the existence

of special vortex configurations in a magnetic field or the coexistence of normal and superconducting regions in the system, where the normal regions may act as weak-links of Josephson junctions and thus lead to an effective geometry with mesoscopic superconducting rings. Since the 0.67 K superconducting phase nucleated near twinning planes still survive below 7.5 kOe, the exotic low field oscillations in Bi wire may have similar origins due to the weak-links of Josephson junction arrays or the combination of superconducting and normal phases in the wire.

We note that samples N2 ($L = 3.0 \mu\text{m}$) and N3 ($L = 2.1 \mu\text{m}$) also showed a superconducting drop in resistance, but the onset of the transition was found near $1.9 \pm 0.2 \text{ K}$ and the resistance drop ended at 75 and 12% of its normal state value, respectively. Although the resistance oscillations below T_c were seen in N2 and N3, no LP-like oscillations can be resolved or identified. LP oscillations require the formation of an unbroken superconducting cylindrical shell around the wire. This is evidently not satisfied in N2 and N3 where the resistance drops incompletely. When the temperature T (or H) approaches T_c (or H_c), the superconductivity in the BiO_x -Bi interfacial region weakens and thus may not form a complete superconducting cylindrical shell around the wire. This may be the reason why the LP oscillations in N1 (Figure 5a) disappear near T_c (or H_c). The SdH-like oscillations were found in N2 and N4 but with different periodicity ($\Delta(1/H) = 0.005 \text{ kOe}^{-1}$ in N2 and $\Delta(1/H) = 0.031 \text{ kOe}^{-1}$ in N4). Since the periodicity of the SdH oscillations inversely depends on the extremal cross-sectional area of the Fermi surface (FS) normal to H , it requires specific alignment of the anisotropic FS with respect to H . While the magnetic field can be aligned to be perpendicular to the axis of the wire, it is not possible to align H with respect to a particular direction of the FS from sample to sample. It is perhaps a fortunate coincidence that in sample N1 the magnetic field is indeed aligned along a specific preferred direction of the FS. We do not fully understand why the best periodicity is found near 0.4 and 0.5 K. It is possible that the less than perfect correlation of the oscillations in N1–N4 with $1/H$ is a consequence of the variations of the FS in the normal regions with respect to applied H and the inhomogeneity of the superconductivity in the wires. Further experiments with well-controlled diameters, orientations and surface oxidation are crucial to clarify the interface-related mysteries observed in Bi nanowires.

In summary, we report the observation of superconductivity in (10 $\bar{1}$ 4) twined Bi nanowire of 72 nm in nominal diameter below 1.3 K. Both Little–Parks-like oscillations in parallel fields and SdH-like oscillations in perpendicular H were found. These data suggest a completely unexpected and novel coexistence of superconducting and metallic states in the surface shell of the Bi nanowire below T_c .

Acknowledgment. We acknowledge helpful discussions with J. Jain, Y. Liu, C. T. Shi, N. Samarth, and J. G. Wang. This work was supported by the Center for Nanoscale Science (Penn State MRSEC) funded by NSF under Grant DMR-0820404, and the Pennsylvania State University Materials Research Institute Nano Fabrication Network and the

References

- (1) Liu, Y.; Allen, R. E. *Phys. Rev. B* **1995**, *52*, 1566.
- (2) Smith, G. E.; Baraff, G. A.; Rowell, J. M. *Phys. Rev.* **1964**, *135*, A1118.
- (3) Hartman, R. *Phys. Rev.* **1969**, *181*, 1070.
- (4) (a) Yang, F. Y.; Liu, K.; Hong, K.; Reich, D. H.; Searson, P. C.; Chien, C. L. *Science* **1999**, *284*, 1335. (b) Yang, F. Y.; Liu, K.; Chien, C. L.; Searson, P. C. *Phys. Rev. Lett.* **1999**, *82*, 3328.
- (5) Yang, F. Y.; Liu, K.; Hong, K. M.; Reich, D. H.; Searson, P. C.; Chien, C. L.; Leprince-Wang, Y.; Yu-Zhang, K.; Han, K. *Phys. Rev. B* **2000**, *61*, 6631.
- (6) Brown, R. D., III *Phys. Rev. B* **1970**, *2*, 928.
- (7) Well, J. W.; Dil, J. H.; Meier, F.; Lobo-Checa, J.; Petrov, V. N.; Osterwalder, J.; Ugeda, M. M.; Fernandez-Torrente, I.; Pascual, J. I.; Rienks, E. D. L.; Jensen, M. F.; Hofmann, Ph. *Phys. Rev. Lett.* **2009**, *102*, 096802.
- (8) Li, L.; Checkelsky, J. G.; Hor, Y. S.; Uher, C.; Hebard, A. F.; Cava, R. J.; Ong, N. P. *Science* **2008**, *321*, 547.
- (9) Behnia, K.; Balicas, L.; Kopelevich, Y. *Science* **2007**, *317*, 1729.
- (10) Fu, L.; Kane, C. L.; Mele, E. J. *Phys. Rev. Lett.* **2007**, *98*, 106803.
- (11) Andrei, B.; Hughes, T. L.; Zhang, S. C. *Science* **2006**, *314*, 1757.
- (12) Hsieh, D.; Qian, D.; Wray, L.; Xia, Y.; Hor, Y. S.; Cava, R. J.; Hasan, M. Z. *Nature* **2008**, *452*, 970.
- (13) Zhang, Z. B.; Sun, X. Z.; Dresselhaus, M. S.; Ying, J. Y.; Heremans, J. *Phys. Rev. B* **2000**, *61*, 4850.
- (14) Hoffman, C. A.; Meyer, J. R.; Bartoli, F. J.; Di Venere, A.; Yi, X. J.; Hou, C. L.; Wang, H. C.; Ketterson, J. B. *Phys. Rev. B* **1993**, *48*, 11431.
- (15) Nikolaeva, A.; Gitsu, D.; Konopko, L.; Graf, M. J.; Huber, T. E. *Phys. Rev. B* **2008**, *77*, 075332.
- (16) (a) Huber, T. E.; Nikolaeva, A.; Gitsu, D.; Konopko, L.; Foss, C. A., Jr.; Graf, M. J. *Appl. Phys. Lett.* **2004**, *84*, 1326. (b) Huber, T. E.; Nikolaeva, A.; Gitsu, D.; Konopko, L.; Graf, M. J. *Physica E* **2007**, *37*, 194.
- (17) Huber, T. E.; Celestine, K.; Graf, M. J. *Phys. Rev. B* **2003**, *67*, 245317.
- (18) Heremans, J.; Thrush, C. M.; Lin, Y. M.; Cronin, S.; Zhang, Z.; Dresselhaus, M. S.; Mansfield, J. F. *Phys. Rev. B* **2000**, *61*, 2921.
- (19) Heremans, J.; Thrush, Zhang, Z.; Sun, X.; Dresselhaus, M. S.; Ying, J. Y.; Morelli, D. T. *Phys. Rev. B* **1998**, *58*, R10091.
- (20) Liu, K.; Chien, C. L.; Searson, P. C. *Phys. Rev. B* **1998**, *58*, R14681.
- (21) Tian, M. L.; Wang, J. G.; Kumar, N.; Han, T. H.; Kobayashi, Y.; Liu, Y.; Mallouk, T. E.; Chan, M. H. W. *Nano Lett.* **2006**, *6*, 2773.
- (22) Tian, M. L.; Kumar, N.; Chan, M. H. W.; Mallouk, T. E. *Phys. Rev. B* **2008**, *78*, 045417.
- (23) Aharonov, Y.; Bohm, D. *Phys. Rev.* **1959**, *115*, 485.
- (24) Degtyareva, O.; McMahon, M. I.; Nelmes, R. J. *High Pressure Res.* **2004**, *24*, 319.
- (25) (a) Little, W. A.; Parks, R. D. *Phys. Rev. Lett.* **1962**, *9*, 9. (b) Parks, R. D.; Little, W. A. *Phys. Rev.* **1964**, *133*, A97.
- (26) Liu, Y.; Zadorozhny, Yu.; Rossario, M. M.; Rock, B. Y.; Carrigan, P. T.; Wang, H. *Science* **2001**, *294*, 2332.
- (27) Tian, M. L.; Xu, S. Y.; Wang, J. G.; Kumar, N.; Wertz, E.; Li, Q.; Campbell, P. M.; Chan, M. H. W.; Mallouk, T. E. *Nano Lett.* **2005**, *5*, 967.
- (28) Li, L.; Zhang, Y.; Li, G. H.; Wang, X. W.; Zhang, L. D. *Mater. Lett.* **2005**, *59*, 1223.
- (29) Valizadeh, S.; Abid, M.; Hernandez-Ramirez, F.; Rodriguez, A. R.; Hjort, K.; Schweitz, A. *Nanotechnology* **2006**, *17*, 1134.
- (30) Cornelius, T. W.; Toimil-Molares, M. E.; Neumann, R.; Karim, S. *J. Appl. Phys.* **2006**, *100*, 114307.
- (31) Tian, M. L.; Wang, J. G.; Kurtz, J. S.; Liu, Y.; Chan, M. H. W.; Mayer, T. S.; Mallouk, T. E. *Phys. Rev. B* **2005**, *71*, 104521.
- (32) Rogachev, A.; Bezryadin, A. *Appl. Phys. Lett.* **2003**, *83*, 512.
- (33) Altomare, F.; Chang, A. M.; Melloch, M. R.; Hong, Y. G.; Tu, C. W. *Phys. Rev. Lett.* **2006**, *97*, 017001.
- (34) Ye, Z. X.; Zhang, H.; Liu, H. D.; Wu, W. H.; Luo, Z. P. *Nanotechnology* **2008**, *19*, 085709.
- (35) Schmidt, V. V. *The physics of superconductors: Introduction to fundamentals and applications*; Muller, P., Ustinov, A. V., Eds.; Springer: New York, 1997.
- (36) Buisson, O.; Gandit, P.; Rammal, R.; Wang, Y. Y.; Pannetier, B. *Phys. Lett. A* **1990**, *150*, 36.
- (37) Bezryadin, A.; Ovchinnikov, Yu, N.; Pannetier, B. *Phys. Rev. B* **1996**, *53*, 8553.
- (38) Moshchalkov, V. V.; Gielen, L.; Strunk, C.; Jonckheere, R.; Qiu, X.; van Haesendonck, C.; Bruynseraede, Y. *Nature (London)* **1995**, *373*, 319.
- (39) Geim, A. K.; Grigorieva, I. V.; Dubonos, S. V.; Lok, J. G. S.; Maan, J. C.; Filippov, A. E.; Peeters, F. M. *Nature (London)* **1997**, *390*, 259.
- (40) Kanda, A.; Baelus, B. J.; Peeters, F. M.; Kadowaki, K.; Ootuka, Y. *Phys. Rev. Lett.* **2004**, *93*, 257002.
- (41) Grigorieva, I. V.; Escoffier, W.; Misko, V. R.; Baelus, B. J.; Peeters, F. M.; Vinnikov, L. Y.; Dubonos, S. V. *Phys. Rev. Lett.* **2007**, *99*, 147003.
- (42) (a) Khaikin, M. S.; Khlyustikov, I. N. *JETP Lett.* **1981**, *33*, 158. (b) Khlyustikov, I. N.; Khaikin, M. S. *JETP Lett.* **1981**, *34*, 198. (c) Khlyustikov, I. N. *J. Exp. Theor. Phys.* **2006**, *102*, 258.
- (43) Suslov, I. M. *Sov. Phys. JETP* **1989**, *68*, 546.
- (44) Averin, V. V.; Buzdin, A. I.; Bulaevskii, L. N. *Sov. Phys. JETP* **1983**, *57*, 426.
- (45) Bezryadin, A.; Lau, C. N.; Tinkham, M. *Nature (London)* **2000**, *404*, 971.
- (46) Lau, C. N.; Markovic, N.; Bockrath, M.; Bezryadin, A.; Tinkham, M. *Phys. Rev. Lett.* **2001**, *87*, 217003.
- (47) Zgirski, M.; Riikonen, K. P.; Touboltsev, V.; Arutyunov, K. *Nano Lett.* **2005**, *5*, 1029.
- (48) Bae, M. H.; Dinsmore III, R. C.; Aref, T.; Brenner, M.; Bezryadin, A. *Nano Lett.* **2009**, *9*, 1889.
- (49) Wosnitza, J.; Wanka, S.; Hagel, J.; Haussler, R.; Lohneysen, H. V.; Schlueter, J. A.; Geiser, U.; Nixon, P. G.; Winter, R. W.; Gard, G. L. *Phys. Rev. B* **2000**, *62*, R11973.
- (50) Doiron-Leyraud, N.; Proust, C.; LeBoeuf, D.; Levallois, J.; Bonne-maison, J. B.; Liang, R.; Bonn, D. A.; Hardy, W. N.; Taillefer, L. *Nature (London)* **2007**, *447*, 565.
- (51) Van der Zant, H. S. J.; Webster, M. N.; Romijn, J.; Mooij, J. E. *Phys. Rev. B* **1994**, *50*, 340.
- (52) Johansson, A.; Sambandamurthy, G.; Shahar, D.; Jacobson, N.; Tenne, R. *Phys. Rev. Lett.* **2005**, *95*, 116805.
- (53) Herzog, A. V.; Xiong, P.; Dynes, R. C. *Phys. Rev. B* **1998**, *58*, 14199.
- (54) Patel, U.; Avci, S.; Xiao, Z. L.; Hua, J.; Yu, S. H.; Ito, Y.; Divan, R.; Ocola, L. E.; Zheng, C.; Claus, H.; Hiller, J.; Welp, U.; Miller, D. J.; Kwok, W. K. *Appl. Phys. Lett.* **2007**, *91*, 162508.
- (55) Wang, J.; Ma, X. C.; Lu, L.; Jin, A. Z.; Gu, C. Z.; Xie, X. C.; Jia, J. F.; Chen, X.; Xue, Q. K. *Appl. Phys. Lett.* **2008**, *92*, 233119.

NL901431T